AIP Conference Proceedings

RESEARCH ARTICLE | NOVEMBER 19 2021

Structure and crystallization of an amorphous film of variable thickness Bi_2Te_3 with a copper sublayer under the action of an electron beam in TEM

V. Yu. Kolosov; A. A. Yushkov

Check for updates

AIP Conf. Proc. 2388, 020012 (2021)
https://doi.org/10.1063/5.0070532

View Online
Export Citation

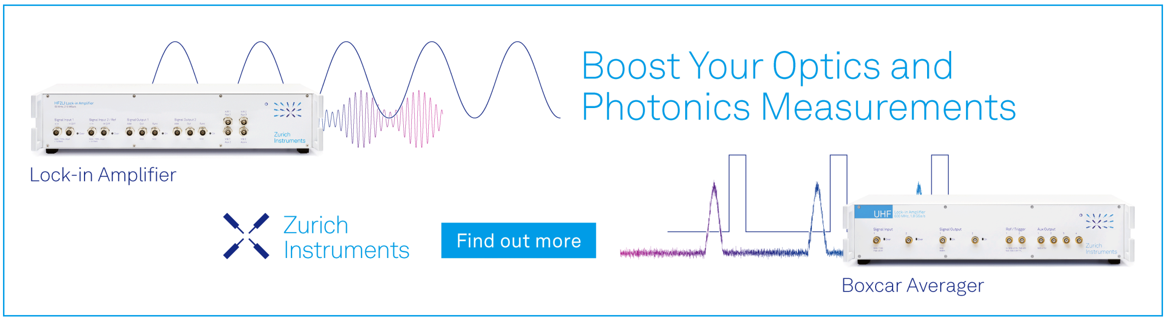

AIP Publishing

22 April 2024 07:30:09

Structure and Crystallization of an Amorphous Film of Variable Thickness Bi_2Te_3 with a Copper Sublayer Under the Action of an Electron Beam in TEM

V. Yu Kolosov[a)], A. A. Yushkov

Ural Federal University, Lenina Av. 51, Ekaterinburg, 620000, Russian Federation.

[a)]Corresponding author: emlab@urfu.ru

Abstract. Nanothin films of bismuth telluride Bi_2Te_3 were obtained by thermal sputtering in vacuum on a mica substrate with amorphous carbon and a copper sublayer. A sample with a specially created sharp thickness gradient was studied by transmission electron microscopy (TEM). An island-labyrinth structure of the film was revealed, with the size of islands in the range of about 7-25 nm. The film is amorphous at the beginning of the thickness gradient; in the studied regions of greater thickness, it crystallizes in the rhombohedral Bi_2Te_3 phase. High-resolution TEM has revealed crystallization of initially amorphous islands under the action of a focused electron beam of increased intensity in an electron microscope column.

INTRODUCTION

Nanothin and island films of chalcogenide materials are attracting increasing interest due to the variety of functional applications determined, in particular, by their microstructure. Bismuth telluride is widely studied as a thermoelectric [1-3], a topological insulator [4, 5], in photoelectrochemistry [6], the production of superconductors [7] and phase transition memory [8]. Structural studies by transmission electron microscopy (TEM) and electron diffraction (ED) of Bi_2Te_3 films were carried out on a JEM-2100 (200 kV).

SAMPLE PREPARATION AND METHODOLOGY

The sample was vacuum deposited on a mica substrate coated with a thin layer of carbon, on a copper sublayer, and separated from the substrate on a TEM grid. An area with a specially created sharp gradient of thickness [9] was investigated to study its effect on the microstructure, Figure 1. Also of interest was the possible effect of a pre-deposited copper sublayer in comparison with Bi_2Te_3 films studied earlier [9], since the effect of amorphization was established during vacuum deposition of Te on a copper sublayer [10] followed by the growth of unusual Te microcrystals [11] with an internal curvature of the crystal lattice planes (called transrotational [12]), which depends, in particular, on the film thickness [13], and on the relative Te content in the film [14]). The sample was investigated by bright field transmission electron microscopy, selected area electron diffraction (SAED), and high-resolution electron microscopy (HREM). The film was exposed by a focused high-intensity electron beam, including *in situ* observations. The electron diffraction patterns were measured using the ImageJ software.

Modern Synthetic Methodologies for Creating Drugs and Functional Materials (MOSM2020)
AIP Conf. Proc. 2388, 020012-1–020012-7; https://doi.org/10.1063/5.0070532
Published by AIP Publishing. 978-0-7354-4142-2/$30.00

22 April 2024 07:30:09

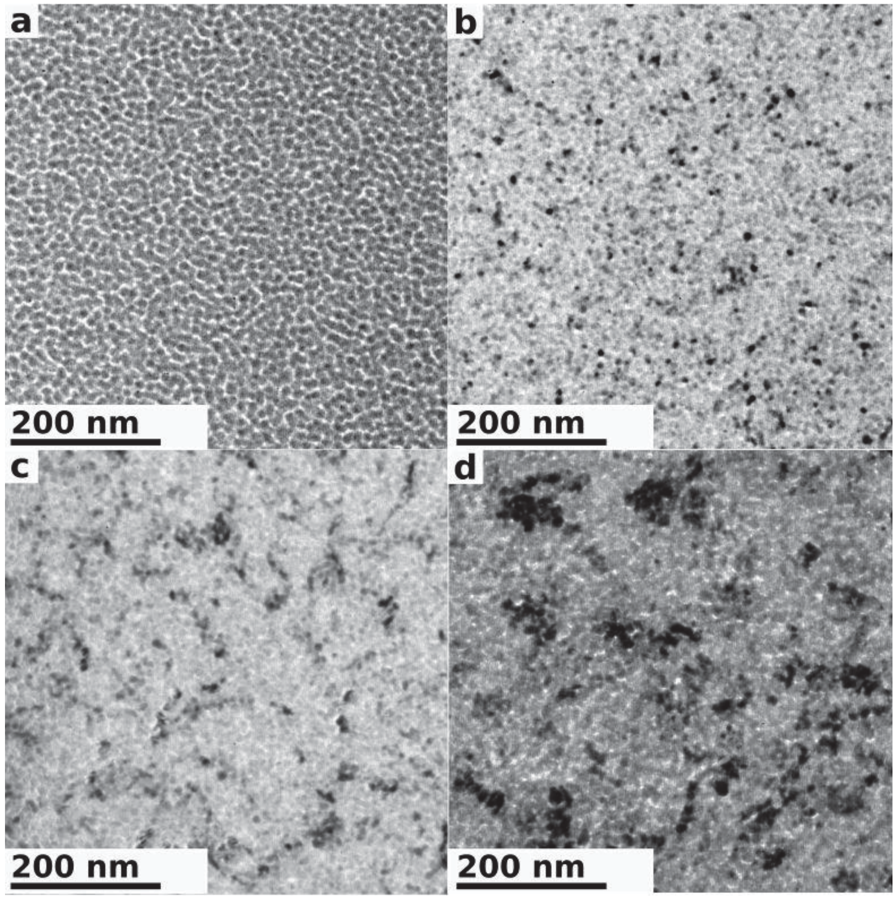

FIGURE 1. TEM images of film regions of a Bi_2Te_3 + Cu sample in different regions of the thickness gradient. a - an image of the area of the smallest thickness, the film is amorphous; b - an image of the transitional amorphous-crystalline region; c - an image of a predominantly crystalline region; d - an image of the crystalline area of the greatest thickness.

RESULTS

In the region of the smallest thickness, the film has an island-labyrinth structure, Figure 2a, 2c, diffraction contrast does not appear, SAED is an amorphous halo, Figure 2b. The sizes of the islands are within 7 - 25 nm in both the amorphous and fine-crystalline regions. Ongoing to large thicknesses, a diffraction contrast in grain orientation appears, Figure 2c, SAED is a fine-crystalline ring pattern, Fig. 2d.

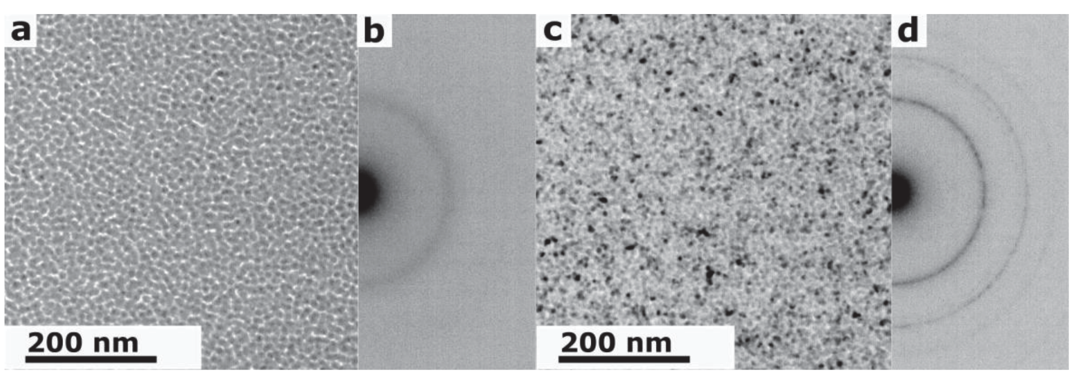

FIGURE 2. a - TEM of a section of the Bi_2Te_3 + Cu film at the beginning of the thickness gradient; b - SAED of the area on the Fig. 2 a; c - film image in the area of greater thickness along the gradient; d - SAED of the area on the Figure 2c.

22 April 2024 07:30:09

During the study, the sample was exposed to a focused high-intensity electron beam, Figure 3. On the film, a change in contrast is noticeable after exposure to a beam, the erasure of the boundaries of individual islands of the island-labyrinth structure

.

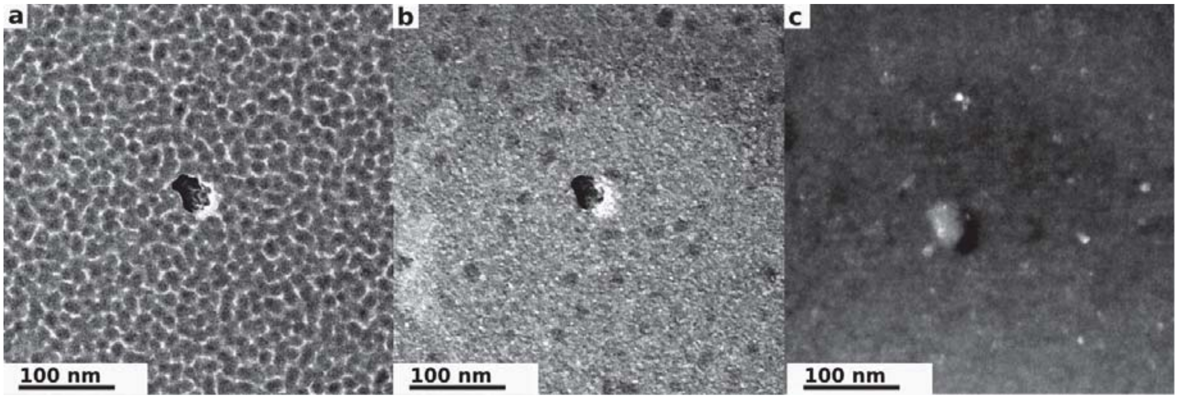

FIGURE 3. a - a section of the initially amorphous film before exposure to the electron beam; b - area after exposure; c - dark-field image (with the capture of a part of the amorphous halo by the objective diaphragm) of the area in Fig. 3b, individual crystallized particles in an amorphous matrix are visible

The profile of the island-labyrinth structure was surveyed at the fold of the film in the middle part of the thickness gradient, Fig. 4. The height of the island profile was estimated within 5 - 8 nm.

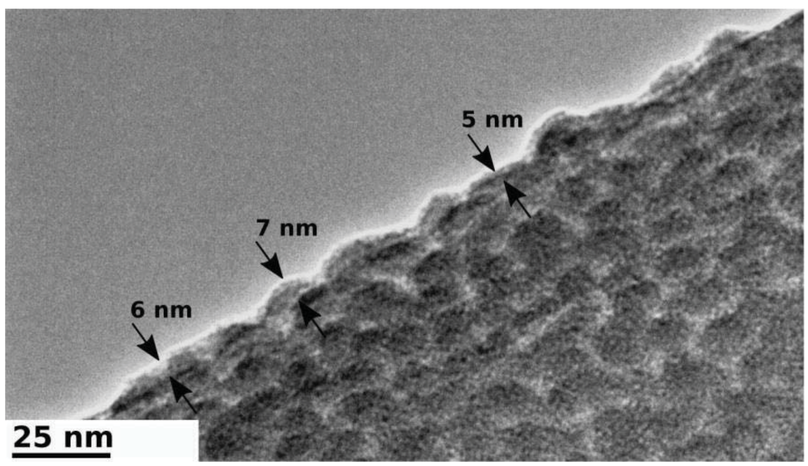

FIGURE 4. TEM image of the fold of the sample film. Arrows indicate examples of measurements of the structure profile height.

During the HREM imaging, crystallization of initially amorphous islands was observed under the action of a highly focused electron beam, Figure 5, 6. The growth of the initially crystalline regions was also observed, Figure 7.

22 April 2024 07:30:09

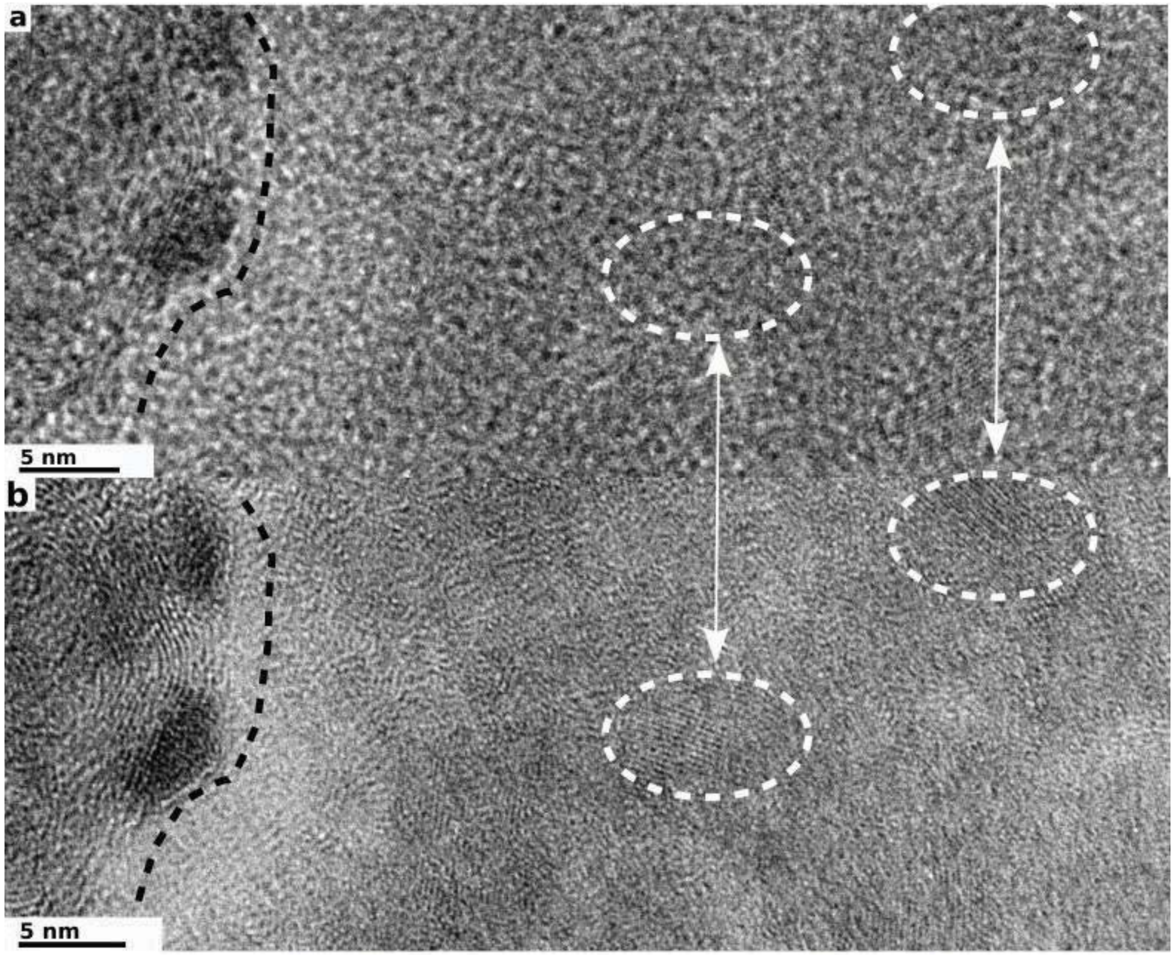

FIGURE 5. HREM of an amorphous film section at the beginning of the thickness gradient before (a) and after exposure to the electron beam (b). White dashed ellipses mark the zones of in situ crystallization (additionally connected by arrows in the "before" and "after" images), black dotted lines indicate the border of the reference area

22 April 2024 07:30:09

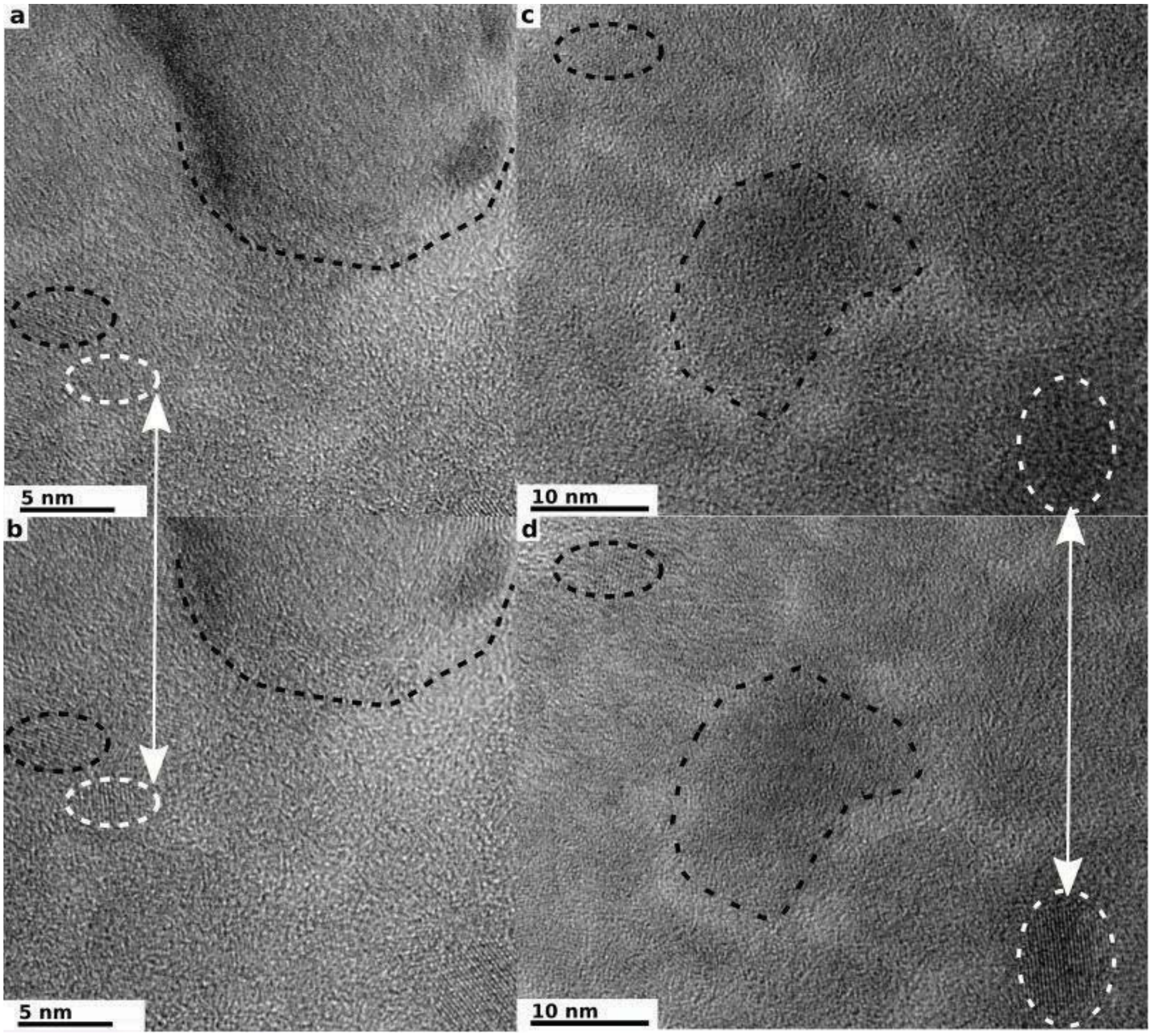

FIGURE 6. HREM of an amorphous film section at the beginning of the thickness gradient before (a, b) and after exposure to the beam (c, d). White dashed ellipses mark the zones of incipient nanocrystals, black - reference regions

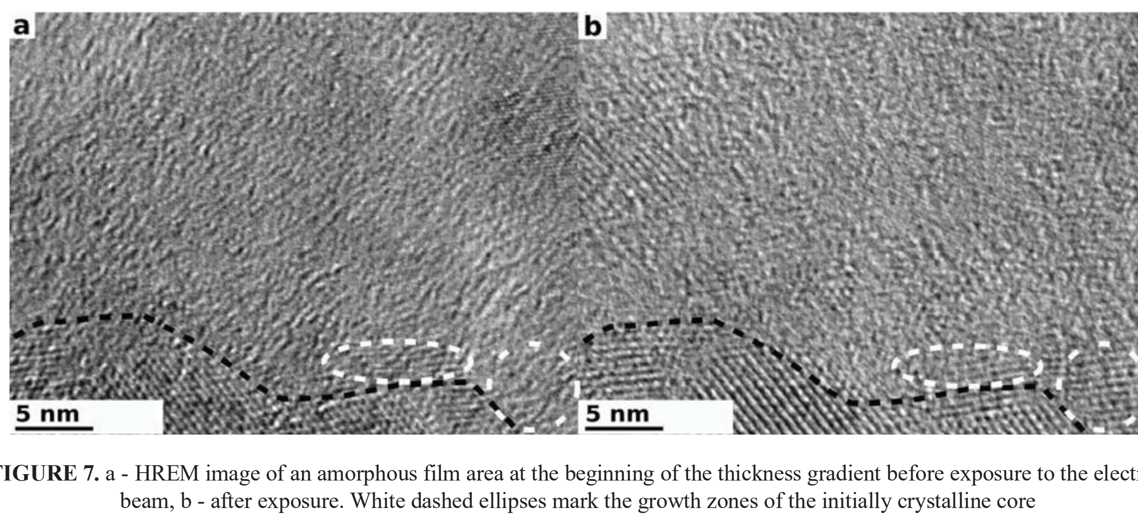

FIGURE 7. a - HREM image of an amorphous film area at the beginning of the thickness gradient before exposure to the electron beam, b - after exposure. White dashed ellipses mark the growth zones of the initially crystalline core

22 April 2024 07:30:09

The ring pattern SAEDs obtained in the thinnest (Figure 8, Table 1) and the thickest (Figure 9, Table 2) areas of the film. The interplanar spacings d_{hkl} were obtained from the diameters of the diffraction rings L measured on the SAED and compared with the JCPDS base. The phase of rhombohedral Bi_2Te_3 (JCPDS 15-0863) was determined.

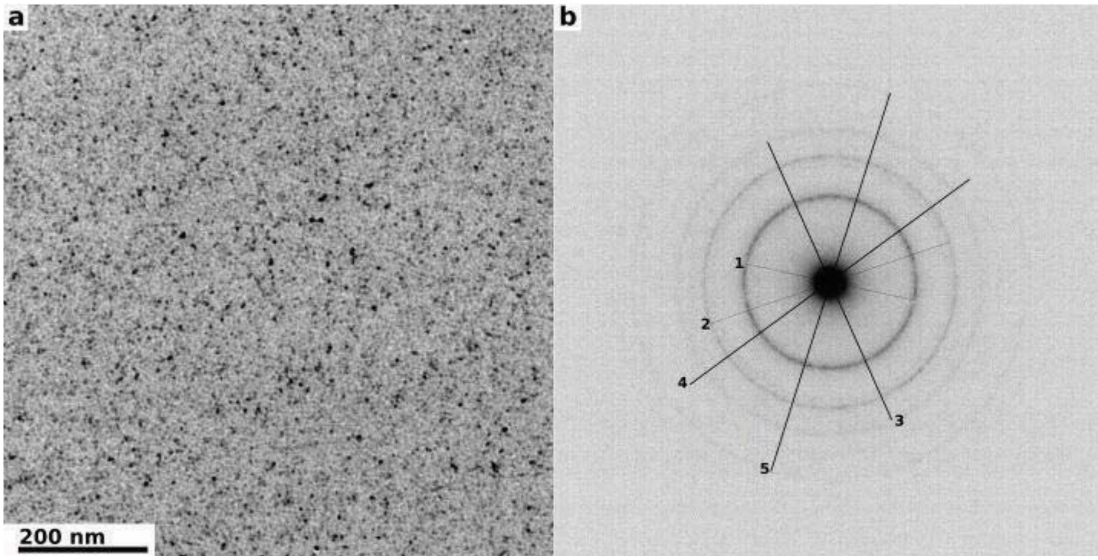

FIGURE 8. a - TEM of a fine-crystalline film region at the beginning of the thickness gradient, b - SAED region in Fig. 8 a with marked diffraction rings

TABLE 1. Indexing of SAED in Figure 8b

L, 1\nm	d_{hkl}, A	Int	d_{hkl} card, A	hkl card	Int card
6,26	3,19	100	3,23	0 1 5	100
9,23	2,17	50	2,21	1 1 0	50
11,08	1,81	30	1,81	2 0 5	30
14,43	1,39	10	1,41	1 2 5	40
12,63	1,58	10	1,61	0 2 10	20

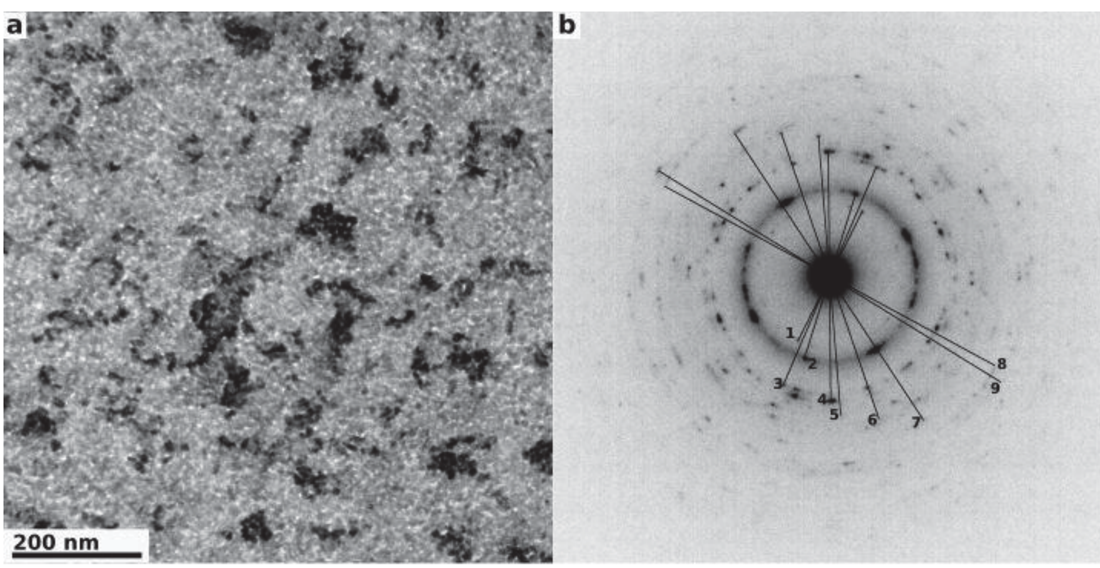

FIGURE 9. a - TEM of a fine-crystalline region of the greatest thickness, b - SAED region in Fig. 9 a with marked diffraction rings

22 April 2024 07:30:09

TABLE 2. Indexing of SAED in Figure 9b

L, 1\nm	d_{hkl}, A	Int	d_{hkl} card, A	hkl card	Int card
5,23	3,82	10	3,83	1 0 1	5
6,3	3,17	100	3,23	0 1 5	100
8,64	2,31	30	2,36	1 0 10	70
9,12	2,19	30	2,21	1 1 0	50
10,21	1,96	10	2	0 0 15	30
11,02	1,81	10	1,81	2 0 5	30
12,52	1,60	10	1,61	0 2 10	20
13,68	1,46	10	1,49	1 1 15	30
14,66	1,36	10	1,41	1 2 5	40

It should be noted that other bismuth tellurides (BiTe JCPDS 15-0820, 31-0200, Bi_4Te_3 JCPDS 33-0216, Bi_3Te_4 JCPDS 38-0458) usually have rather close d_{hkl} data and their presence cannot be ruled out. In addition, there could be an overlap of copper reflections with close values of some d_{hkl}.

CONCLUSION

Vacuum deposited bismuth telluride Bi_2Te_3 is deposited on a carbon substrate with a copper sublayer in the form of an island-labyrinth structure, with island sizes ranging from 7 to 25 nm. In the presence of a sharp thickness gradient, in the regions of the smallest thickness, the film is initially amorphous. The study of areas of greater thickness revealed a crystal microstructure, which can be attributed to the phase of rhombohedral Bi_2Te_3. The film shows a tendency to change in morphology under the action of a focused electron beam of increased intensity: a change in the contrast and the boundaries of the islands. In the high-resolution imaging mode, in situ crystallization of initially amorphous islands was observed, as well as the growth of initially crystalline cores. The significant effect of the copper sublayer at this stage of the study was not recorded.

22 April 2024 07:30:09

ACKNOWLEDGMENTS

Partial financial support from the RFBR grants 19-32-90255, 20-02-00906 and FEUZ-2020-0051 project are acknowledged.

REFERENCES

1. H. Mamura, M. R. A. Bhuiyana, F. Korkmazb and M. Nil, Renewable and Sustainable Energy Reviews **82**, 4159-4169 (2018).
2. D. Champier, Energy Conversion and Management **140**, 167-181 (2017).
3. H. Choi, K. Jeong, Nano Energy **47**, 374-384 (2018).
4. J. Kampmeier, C. Weyrich, Journal of Crystal Growth **443**, 38-42 (2016).
5. P. H. Le, P.-T. Liu, C. W. Luo, J.-Y. Lin and K. H. Wu, Journal of Alloys and Compounds, **692**, 972-979 (2017).
6. J. B. Thorat, S. V. Mohite, Materials Science in Semiconductor Processing **79**, 119-126 (2018).
7. S. G. Buga, V. A. Kulbachinskii, Chem. Phys. Lett. **631–632**, 97-102 (2015).
8. K. Ren, R. Li et al., Journal of Alloys and Compounds, **754**, 227-231 (2018).
9. V. Yu Kolosov, A. A. Yushkov, "Microstructures in thin Bi_2Te_3 films according to transmission electron microscopy", AIP Conference Proceedings, **2313**, 030019 (2020).
10. I. E. Bolotov and A. V. Kozhin, Sov. Phys.-Solid State (in Russian) **15**, 436-38 (1973).
11. I. E. Bolotov, V. Yu. Kolosov, A. V. Kozhin, Phys. Stat. Sol. **72a**, 645-654 (1982).
12. V. Yu. Kolosov, A. R. Thölen, Acta Mater. **48**, 1829-1840 (2000).
13. V. Yu. Kolosov, A. V. Kozhin, L. V. Veretennikov, C. L. Schwamm, "Transrotational crystals growing in amorphous Cu-Te film", In: Richter S., Schwedt A. (eds) EMC 2008 14th European Microscopy Congress 1–5 September 2008, Aachen, Germany. Springer, Berlin, Heidelberg.
14. V. Yu. Kolosov and C. L. Schwamm, AIP Conference Proceedings **2280**, 040022 (2020),